Supplementary Material

Publisher: Elsevier

Journal: Environmental Modelling & Software

DOI: 10.1016/j.envsoft.2021.105118

The following Supplementary Material is available for this article:

Figure S5. The LC-excess profiles for Plausibility Tests 3-6 at 250 d obtained using fine spatial discretization.

Figure S6. The temporal distribution of precipitation (a), evapotranspiration (b), soil surface temperature (c), and air humidity (d) during the simulation period for the *Stumpp et al.* (2012) dataset.

Method S1. Estimation of the atmospheric isotope ratio R_a.

Tables

Table S1. Equations used in this study to calculate the kinetic fractionation coefficient (n_k).

Comment	Formulation	References
Molecular diffusion only	$\alpha_i^k = \frac{D_v}{D_i^v}$, i.e. n_k=1	*Barnes and Allison* (1983, 1984)
The evolution from molecular to turbulent transfer	$\alpha_i^k = (\frac{D_v}{D_i^v})^{n_k}$, $n_k = \frac{(\theta_s-\theta_r)n_a+(\theta_{sat}-\theta_s)n_s}{(\theta_{sat}-\theta_r)}$ $n_a = 0.5,\ n_s = 1,$ $\theta_s,\ \theta_{sat}$, and θ_r are the volumetric water contents at the soil surface, the saturated water content, and the residual water content, respectively.	*Mathieu and Bariac* (1996)
Turbulent transfer only	$\alpha_i^k = 1$, i.e. n_k=0	*Melayah et al.* (1996a)

Table S2. Optimized soil hydraulic and solute transport parameters from *Stumpp et al.* (2012).

Horizon	Depth	θ_r	θ_s	α	n	K_s	Λ
	cm			cm^{-1}	-	cm/d	cm
Ap	0–30	0	0.30	0.023	1.140	110	4.7
Bv	31–90	0	0.32	0.076	1.070	6000	4.7
Cv	91–150	0	0.32	0.016	1.900	110	4.7

Table S3. Estimated flow parameters for each particle during the simulation period.

Particle Number	Initial Release Time (day)	Final Exit Time (day)	Transit Time (day)	Mean velocity (mm/day)
19	9.2955	190.8045	181.51	8.26
20	34.39	193.25	158.86	9.44
21	94.53	237.10	142.57	10.52
22	101.14	305.61	204.47	7.34
23	143.29	519.76	376.47	3.98
24	182.37	547.03	364.66	4.11
25	216.63	697.37	480.74	3.12
26	305.00	759.61	454.61	3.30
27	484.67	825.00	340.33	4.41
28	522.80	874.76	351.96	4.26
29	694.29	946.13	251.84	5.96
30	759.17	1054.13	294.96	5.09
31	801.80	1055.68	253.88	5.91
32	845.46	1162.78	317.32	4.73
33	873.74	1205.40	331.66	4.52
34	944.80	1325.61	380.81	3.94
35	1054.77	1357.25	302.48	4.96
36	1161.38	1423.88	262.50	5.71
37	1170.37	1425.82	255.45	5.87
38	1199.00	1484.65	285.65	5.25
39	1313.80	1514.00	200.20	7.49
40	1356.22	1581.16	224.94	6.67
41	1424.64	1652.80	228.16	6.57
42	1484.35	1663.10	178.75	8.39
43	1525.21	1710.63	185.42	8.09
44	1556.32	1723.48	167.16	8.97
Mean			276.05	6.03

Table S4. Comparison of the water storage in the soil profile when the particle leaves the transport domain at its bottom with the net water input into the soil profile during particle's presence in the profile.

Particle number	Final water storage (cm)	Precipitation (cm)	Actual evaporation (cm)	Actual transpiration (cm)	Net water input since particle release (cm)	Absolute error (cm)	Relative error (%)
19	39.42	79.84	34.51	5.91	39.42	0.00	0.00
20	39.64	72.56	27.68	5.29	39.59	0.05	0.12
21	40.06	53.49	11.55	1.91	40.03	0.03	0.07
22	40.21	51.65	11.15	0.56	39.94	0.27	0.67
23	41.30	94.64	43.40	10.18	41.07	0.24	0.58
24	39.34	91.03	41.70	10.00	39.33	0.01	0.03
25	40.94	90.56	41.63	8.14	40.78	0.15	0.37
26	40.44	98.38	54.16	4.07	40.15	0.28	0.70
27	35.89	79.47	35.18	8.64	35.65	0.24	0.67
28	40.67	90.57	38.53	11.78	40.25	0.42	1.03
29	39.72	90.87	40.34	10.86	39.67	0.05	0.13
30	41.00	76.02	27.84	7.22	40.95	0.04	0.10
31	41.35	59.16	16.24	1.78	41.14	0.21	0.50
32	39.70	76.02	33.27	3.13	39.62	0.07	0.18
33	39.96	88.08	34.21	14.06	39.81	0.15	0.38
34	40.35	97.04	43.01	13.86	40.17	0.18	0.44
35	39.44	93.46	43.01	11.06	39.39	0.05	0.13
36	41.30	66.80	18.98	6.74	41.08	0.22	0.53
37	40.91	60.33	17.65	2.02	40.66	0.24	0.60
38	41.07	66.54	25.71	0.13	40.70	0.37	0.90
39	39.33	59.41	19.27	0.95	39.19	0.14	0.37
40	40.72	83.09	31.14	11.41	40.54	0.17	0.42
41	39.87	90.75	40.08	10.90	39.77	0.10	0.25
42	39.28	75.49	28.17	8.05	39.27	0.00	0.01
43	39.23	58.81	17.80	1.83	39.18	0.05	0.12
44	40.20	53.87	13.45	0.45	39.97	0.23	0.58

Figures

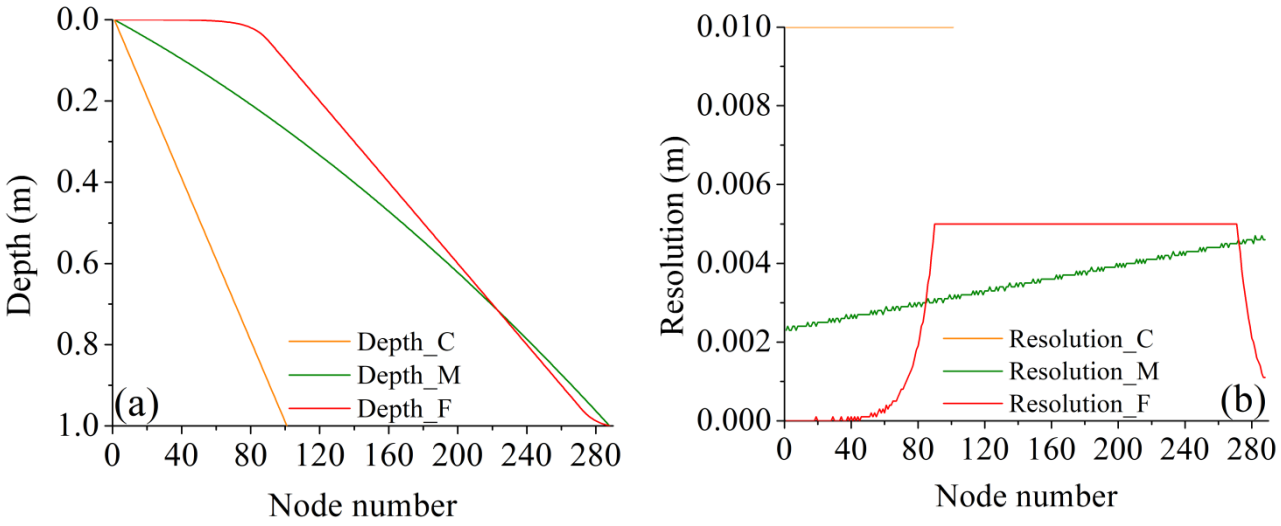

Figure S1. The node distribution versus depth (a) and spatial steps versus the node number (b) for the coarse, medium, and fine spatial discretizations. 'C', 'M', and 'F' refer to 'coarse,' 'medium,' and 'fine', respectively.

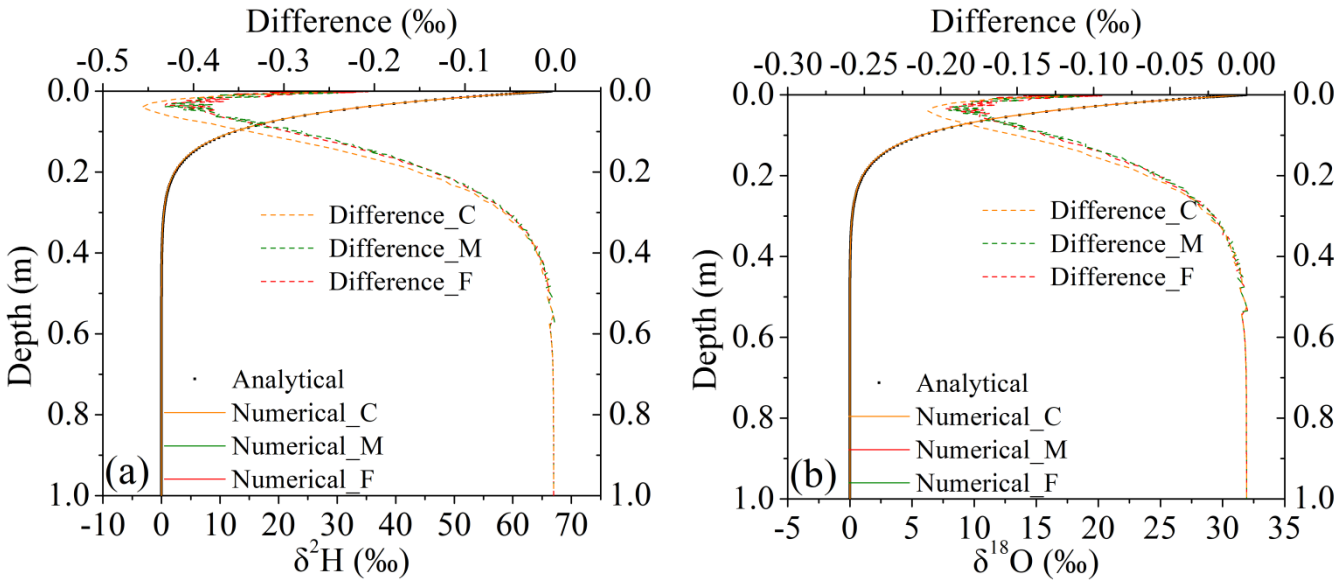

Figure S2. Comparison of analytical and numerical solutions (bottom axis) and their differences (top axis) for (a) ^{2}H and (b) ^{18}O isotopic composition profiles using the coarse, medium, and fine spatial discretizations for isothermal saturated soil under steady evaporation. 'C', 'M', and 'F' refers to 'coarse', 'medium', and 'fine', respectively.

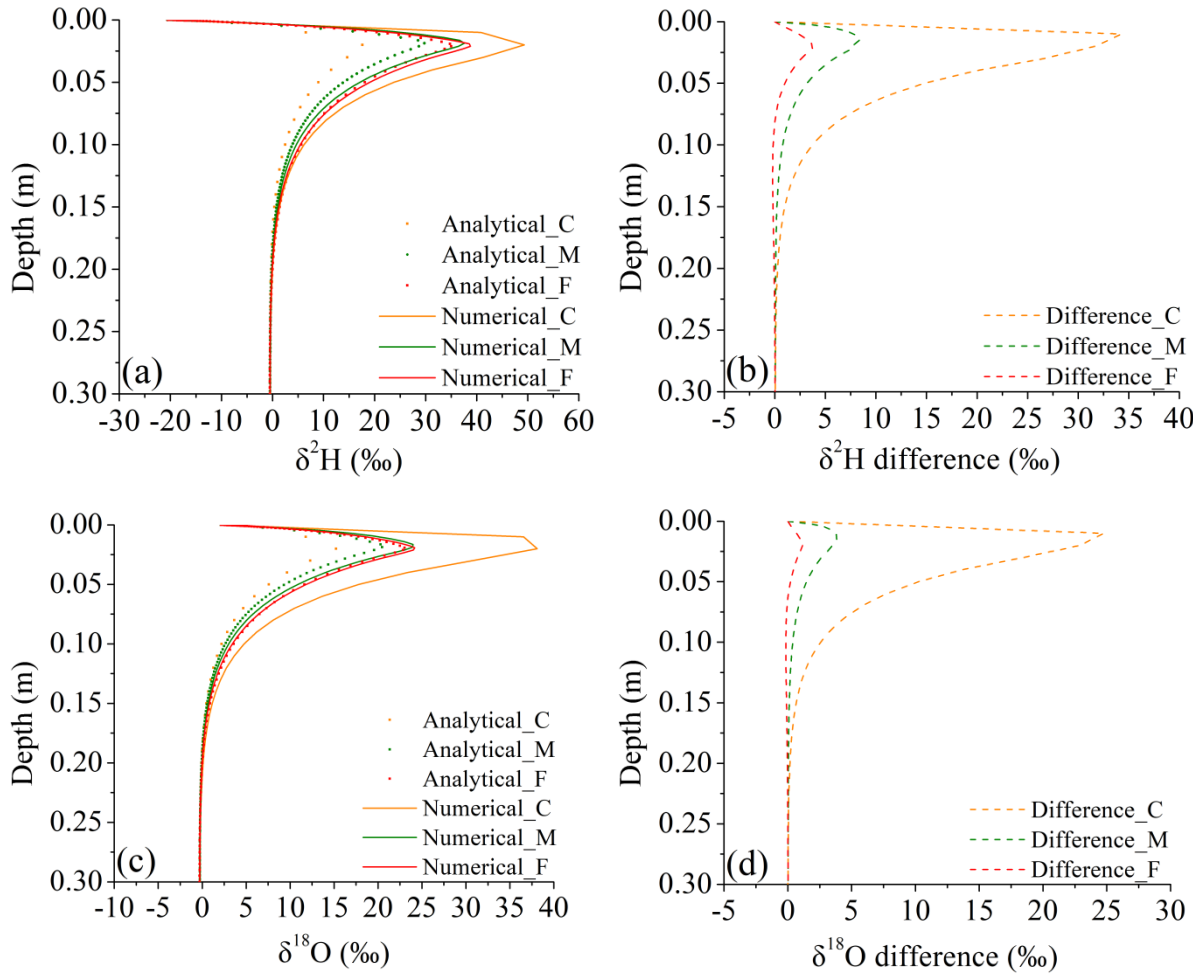

Figure S3. Comparison of analytical and numerical solutions (left) and their differences (right) for ^{2}H (top) and ^{18}O (bottom) isotopic composition profiles using the coarse, medium, and fine spatial discretizations for nonisothermal unsaturated soil under steady evaporation. 'C', 'M', and 'F' refer to 'coarse', 'medium', and 'fine', respectively. Results are presented for the top 30 cm only.

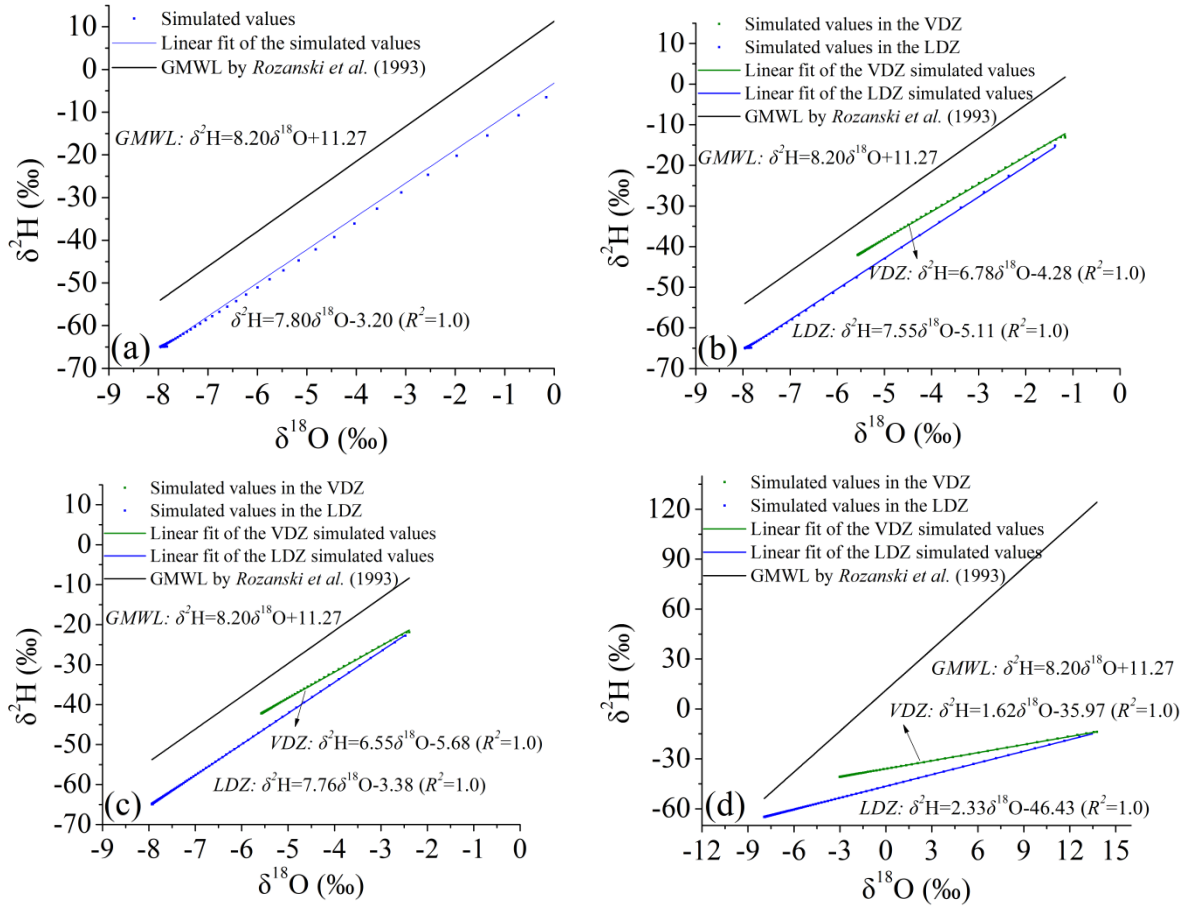

Figure S4. The ^{2}H-^{18}O isotope plots for Plausibility Tests 3-6 (a-d) at 250 d obtained using fine spatial discretization.

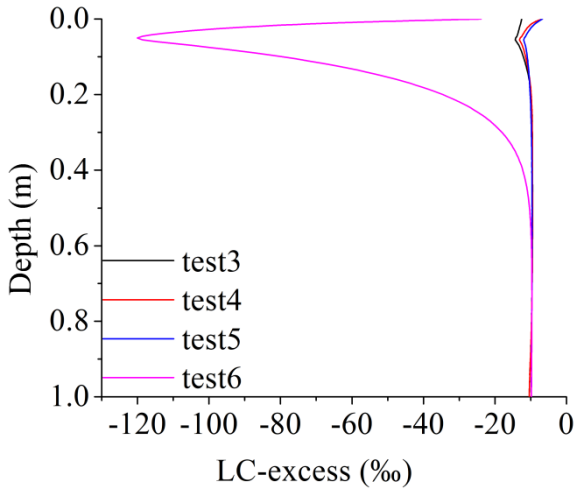

Figure S5. LC-excess profiles for Plausibility Tests 3-6 at 250 d obtained using fine spatial discretization.

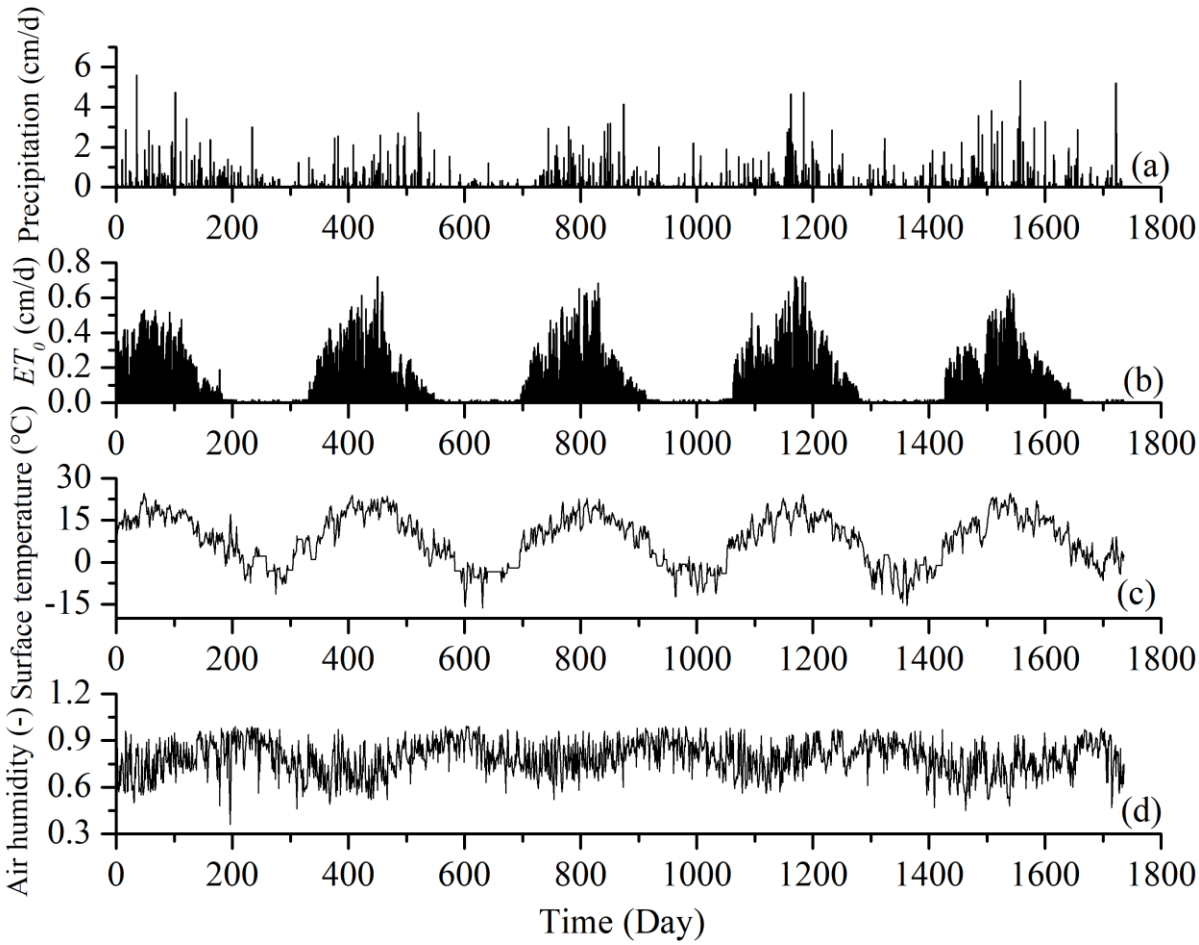

Figure S6. The temporal distribution of precipitation (a), potential evapotranspiration (ET_0) (b), soil surface temperature (c), and air humidity (d) during the simulation period for the *Stumpp et al.* (2012) dataset.

Method S1. Estimation of the atmospheric isotope ratio R_a.

The atmospheric isotope ratio (R_a), an important parameter in the Craig-Gordon model (Eq. 7), is difficult to measure and not always available. It is commonly estimated assuming that its isotopic composition is in equilibrium with that of rainfall (e.g., *Araguás-Araguás et al.*, 2000; *Skrzypek et al.*, 2015; *Benettin et al.*, 2018). However, the equilibrium assumption is mainly used for long-term (e.g., monthly) calculations rather than individual rain events because of various complications on short time scales and local effects. The estimation of R_a from precipitation may not be available for rain-free periods, in arid zones, or areas with significant local or upwind evapotranspiration moisture (*Gibson et al.*, 2008; *Crawford et al.*, 2019). Therefore, the atmospheric isotope ratio was estimated in this study by comparing the measured isotopic compositions with those simulated using the Gonfiantini evaporation fractionation model.

When only equilibrium fractionation is considered (i.e., $\alpha_i^* = \alpha_i^*;\ \ n_k = 0$), which is very common in humid zones, the isotope ratio of the evaporation flux calculated using the Gonfiantini model (Eq. 17) can be simplified as:

$$R_{E\_SWIS} = \frac{R_L}{\alpha_i^{total}} = \alpha_i^* R_L \tag{S1}$$

In humid zones, additional simplifying assumptions can be used: the relative humidity of the soil air phase at the surface equals 1 ($H_{rs} = 1$) and the soil surface and atmospheric temperatures are equal ($T_s = T_a$) (*Gat*, 2010; *Gonfiantini*, 1986). When the R notation is used to define isotope concentrations, the isotope ratio of the evaporation flux calculated using the Craig-Gordon model (Eq. 8) under these conditions can be simplified as follows (*Gat*, 2010):

$$R_{E\_CG} = \frac{\alpha_i^* \cdot R_L - h_a \cdot R_a}{1 - h_a} \tag{S2}$$

Since $R_{E\_CG} > 0$, we have:

$$R_a < \frac{\alpha_i^* \cdot R_L}{h_a} \tag{S3}$$

The difference in the isotope ratio of the evaporation flux evaluated using the Gonfiantini and Craig-Gordon models then is:

$$R_{E\_SWIS} - R_{E\_CG} = \alpha_i^* R_L - \frac{\alpha_i^* \cdot R_L - h_a \cdot R_a}{1 - h_a} = \frac{h_a \cdot (R_a - \alpha_i^* \cdot R_L)}{1 - h_a} \tag{S4}$$

There exist three cases when the Gonfiantini model either overestimates, underestimates, or matches the effects of evaporation fractionation compared to the Craig-Gordon model:

(1) If $R_{E\_SWIS} - R_{E\_CG} < 0$, then:

$$R_a < \alpha_i^* \cdot R_L \tag{S5}$$

(2) If $R_{E\_SWIS} - R_{E\_CG} > 0$, we get using Eq. (S3):

$$\alpha_i^* \cdot R_L < R_a < \frac{\alpha_i^* \cdot R_L}{h_a} \tag{S6}$$

(3) If $R_{E\_SWIS} - R_{E\_CG} = 0$, then:

$$R_a = \alpha_i^* \cdot R_L \tag{S7}$$

This means that only when $R_a = \alpha_i^* \cdot R_L$, we get the same results with both the Gonfiantini or Craig-Gordon models. In the case when fractionation is negligible, the no-fractionation assumption can be used ($\alpha_i^* = 1$), then $R_a = R_L$, and $R_{E\_SWIS} = R_{E\_CG} = R_L$.

If we consider evaporation fractionation ($\alpha_i^* \neq 1$) and want the Craig-Gordon model to have the same results as with no fractionation, then we need to have:

$$R_{E\_CG} = \frac{\alpha_i^* \cdot R_L - h_a \cdot R_a}{1 - h_a} = R_L \tag{S8}$$

Then:

$$R_a = \frac{(\alpha_i^* - 1 + h_a) \cdot R_L}{h_a} \tag{S9}$$

In the field evaluation example (Fig. 6), the isotopic composition's measured values are initially close to the values simulated by the Gonfiantini model without considering fractionation. Later on (about 1150~1500 days), they are close to the values simulated considering equilibrium fractionation. To obtain similar simulation results using the Craig-Gordon model, the early atmospheric isotope ratio R_a should correspond to Eq. (S9), while the late R_a should correspond to Eq. (S7). This indicates that the atmospheric isotope ratio R_a in the entire simulation period should be between these two cases. Therefore, an approximate estimate (the average R_a estimated by Eqs. (S7) and (S9)) was used in this study in the Craig-Gordon model implemented into the HYDRUS isotope module, i.e.:

$$R_a = \frac{(\alpha_i^* - 1 + h_a + h_a \cdot \alpha_i^*) \cdot R_L}{2h_a} \tag{S10}$$

In theory, the atmospheric isotope ratio R_a is determined by the atmosphere above the soil, and therefore, should be independent of what happens in the soil. However, the approach described above can provide a relatively reasonable estimate of R_a to be used in the Craig-Gordon model to fit the measurements.

References

Araguas-Araguas, L., K. Froehlich, and K. Rozanski, Deuterium and oxygen-18 isotope composition of precipitation and atmospheric moisture, *Hydrological Processes*, *14*(8), pp. 1341-1355, doi:10.1002/1099-1085(20000615)14:8<1341::aid-hyp983>3.0.co;2-z, 2000.

Benettin, P., T.H.M. Volkmann, J. von Freyberg, J. Frentress, D. Penna, T.E. Dawson, and J. Kirchner, Effects of climatic seasonality on the isotopic composition of evaporating soil waters, *Hydrology and Earth System Sciences*, *22*(5), pp. 2881-2890, doi:10.5194/hess-22-2881-2018, 2018.

Crawford, J., C.S. Azcurra, C.E. Hughes, J.J. Gibson, and S.D. Parkes, Comparison of atmospheric water vapour delta O-18 and delta H-2 estimated using evaporation pan, rainfall equilibrium and continuous measurements, *Journal of Hydrology*, *576*, pp. 551-560, doi:10.1016/j.jhydrol.2019.06.056, 2019.

Gat, J., Isotope Hydrology: A Study of the Water Cycle, 6, World Scientific, pp., 2010.

Gibson, J.J., S.J. Birks, and T.W.D. Edwards, Global prediction of delta(A) and delta H-2-delta O-18 evaporation slopes for lakes and soil water accounting for seasonality, *Glob. Biogeochem. Cycle*, *22*(2), pp. 12, doi:10.1029/2007gb002997, 2008.

Gonfiantini, R., Environmental isotopes in lake studies, *Handbook of environmental isotope geochemistry*, *2*, pp. 113-168, 1986.

Skrzypek, G., A. Mydlowski, S. Dogramaci, P. Hedley, J.J. Gibson, and P.F. Grierson, Estimation of evaporative loss based on the stable isotope composition of water using Hydrocalculator, *Journal of Hydrology*, *523*, pp. 781-789, doi:10.1016/j.jhydrol.2015.02.010, 2015.